



Preparation of Carbon-Coated TiO₂ Immobilized on Expanded Graphite/Activated Carbon Composite and its Application for Photodegradation of Formaldehyde Gas†

CHENGBAO LIU^{1,2}, JUNCHAO QIAN³, CHENG GU², ZHIGANG CHEN^{1,2,3,*},
FENG CHEN², ZHENG XU³, PING LI², FENGJUAN HE² and ZHENYING WU²

¹Jiangsu Key Laboratory for Environment Functional Materials, Suzhou University of Science and Technology, Suzhou 215009, P.R. China

²School of Chemistry, Biology and Materials Engineering, Suzhou University of Science and Technology, Suzhou 215009, P.R. China

³School of Materials Science and Engineering, Jiangsu University, Zhenjiang 212013, Jiangsu Province, P.R. China

⁴Jiangsu Provincial Key Laboratory for Interventional Medical Devices, Huaiyin Institute of Technology, Huaian 223003, Jiangsu Province, P.R. China

*Corresponding author: E-mail: czg@mail.usts.edu.cn

Published online: 1 March 2014;

AJC-14778

A new material carbon-coated TiO₂ immobilized on expanded graphite/activated carbon composite (C-TiO₂/EGCs) was synthesized to solve indoor air pollution problems. The TiO₂ coated by carbon layer was immobilized on the outer surface of expanded graphite-based carbon/carbon composites EGCs. The porous texture and the microstructure of the composite were analyzed by using nitrogen adsorption-desorption measurements, XRD, SEM and TEM. The influence of conditions on the formaldehyde degradation was investigated. The results indicated that carbon film not only ensured the adsorption performance and realize dv higher photocatalytic degradation ability of formaldehyde.

Keywords: Expanded graphite carbon/carbon composites, Adsorption, Photodegradation, Formaldehyde, Microstructure.

INTRODUCTION

With the improvement of aesthetic and living standards, there are many decorative materials, paint, polymerizing plate and binder of some combination furniture and chemical fiber carpet, *etc.* used to beautify house. The growing uses in building construction have caused serious indoor air pollution problems that they would bring volatile organic compounds (VOCs)^{1,2}. One of the most representative volatile organic compounds is formaldehyde. Formaldehyde is a colourless, pungent-smelling gas known to cause several symptoms and diseases. Long-term exposure to low concentration formaldehyde can cause irritation of the eyes, reddening of the skin, headache, nausea, drowsiness, allergic reactions and possible negative effects on fetal development³. Formaldehyde is suspected to be a human carcinogen^{4,5}. Because of this many countries have set guidelines for the maximum allowable indoor concentrations.

There are some general methods currently used to purify the polluted air such as adsorption and photodegradation⁶. The well known and widely used adsorbents are activated carbons

because of its high specific surface area⁷. However, they are produced in powder or granular form and the pores of the activated carbon are easily occupied by the adsorbate. Moreover, the considerable closed pores in activated carbon reduce the adsorption capacity and the utilization ratio.

Herein, we design a new adsorbent with remarkable photocatalytic activity for photodegradation of formaldehyde. The hierarchical multilayer structure not only enhances the flow of gas, but also improves the efficiency of adsorption. TiO₂ can produce photo-induced electron-hole pairs under the irradiation. From the point view of photo-conversion efficiency, the photocatalytic properties of TiO₂ can be further enhanced if the recombination of the photo-induced electron-hole pairs can be effectively suppressed⁸⁻¹⁰. Expanded graphite-TiO₂ composites are thus promising photocatalytic materials because graphite can act as an electron transfer channel thus reduces the recombination of the photogenerated electron holes¹¹⁻¹⁵. In this paper, we loaded P25 nanoparticles on the platform of a graphite nanosheet and discuss the *situ* photocatalytic regeneration of expanded graphite carbons with the TiO₂ coated.

†Presented at The 7th International Conference on Multi-functional Materials and Applications, held on 22-24 November 2013, Anhui University of Science & Technology, Huainan, Anhui Province, P.R. China

EXPERIMENTAL

Preparation of the EGCs: Expanded graphite was prepared in laboratory according to the previous work. A certain quantity of EG was immersed into the sucrose-phosphoric acid solution with various concentrations under vacuum conditions. The impregnation ratio (weight of H_3PO_4 relative to that of sucrose) was 1.0. Then the material was heated in an electric oven at 80°C for 10 h and solidified at 160°C for 4 h. At the end, the material was carbonized and activated in a pipe stove under nitrogen flow for 2 h. The temperature was controlled in 350°C . The final product was cooled down to room temperature in the nitrogen atmosphere. The sample was rinsed with the ultrapure water until no phosphate ions detected by $\text{Pb}(\text{NO}_3)_4$. It has a bulk density of 4 kg/m^3 and a surface area of $40\text{ m}^2/\text{g}$ (determined by N_2 adsorption at 77K). The sucrose ($\text{C}_{12}\text{H}_{22}\text{O}_{11}$) was dissolved in deionized water with a certain quality concentration and added to a suspension of TiO_2 anatase in water and under ultrasonic oscillation for 0.5 h. Then the EGCs prepared from previous step were immersed into the slurry for 0.5 h. It was then heated at 100°C to evaporate the water in oven and calcinated at 500°C for 2 h with a temperature gradient of $5.0^\circ\text{C}/\text{min}$ that could remove the constitutional water and retain carbon of sucrose.

Analytical procedures: The porous texture characterization of all the samples was carried out by the nitrogen adsorption measurement at 77K (Micromeritics, America). The surface areas have been obtained from the BET equation. The total pore volume has been calculated from the nitrogen gas adsorption capacity at a relative pressure of 0.98. The morphologies of the samples were observed on FESEM microscope (Hitachi S-4800, Japan).

RESULTS AND DISCUSSION

XRD analysis: The diffracted peak at $2\theta = 26.5^\circ$ in the spectrum of the EGCs was the typical graphite crystal (002) characteristic peak. Before 26.5° , there is a characteristic peaks like a hump. This phenomenon indicates amorphous carbon existed in the composite. The peaks at 25.3 , 37.8 and 62.5 are the diffractions of (101), (004) and (204) planes of anatase, indicating the growing TiO_2 existed in anatase state. At $2\theta = 54.9^\circ$, the strengthened peak like a little hill corresponding to the (211) plane of anatase also revealed the existence of amorphous carbon in the composite. The characteristic absorption peak of rutile (110) crystal plane did not appear in Fig. 1.

Electron microscope analysis: Scanning electron microscopic images (Fig. 2(a-d)) clearly demonstrated the multi-layer structure of the C- TiO_2 /EGCs compared to the EGCs. Fig. 2a shows the EGCs without TiO_2 particles. After loading with TiO_2 , the material retains the microscopic structure of the expanded graphite sheet (Fig. 2b) and TiO_2 particles successfully coated on the surface of the EGCs and lamellar structure with scattered distribution (Fig. 2c). From the longitudinal section observation, it can be clearly seen there is little TiO_2 particle existing in central part of C- TiO_2 /EGCs (Fig. 2d). It could mainly attribute to the control of the impregnation process and the TiO_2 particles rarely infiltrate into the central part of the composite material. It could reduce

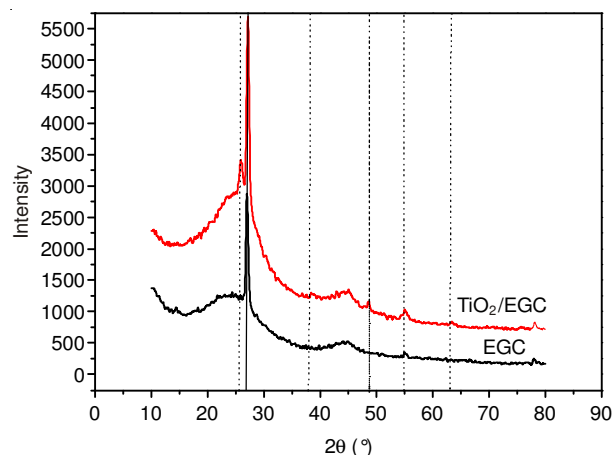


Fig. 1. XRD pattern of EGCs and C- TiO_2 /EGCs

the possibility of a specific surface decrease caused by the pore blocking.

Fig. 2(e) and (f) show the TEM images of C- TiO_2 /EGCs. TiO_2 in EGC surface is relatively scatteredly distributed and coated with a thin layer of carbon membrane. It is especially advantageous to load TiO_2 on EGC surface coated with carbon film by using this way. It is helpful for dispersion of nanoparticles. It can enhance the bond between TiO_2 particles and the substrate surface. In addition, TiO_2 nanoparticles do not aggregate *via* the high temperature treatment and can restrain TiO_2 crystal transition at the same time. Furthermore, it improves the photocatalytic activity of TiO_2 because of carbon element doped effect. Fig. 2(f) display that TiO_2 nanoparticles size are 20 nm. Due to the nanometer quantum size effect, the conduction band and valence band level split into discrete level to obtain a strong reduction and oxidation capacity and ensure its strong light catalytic activity.

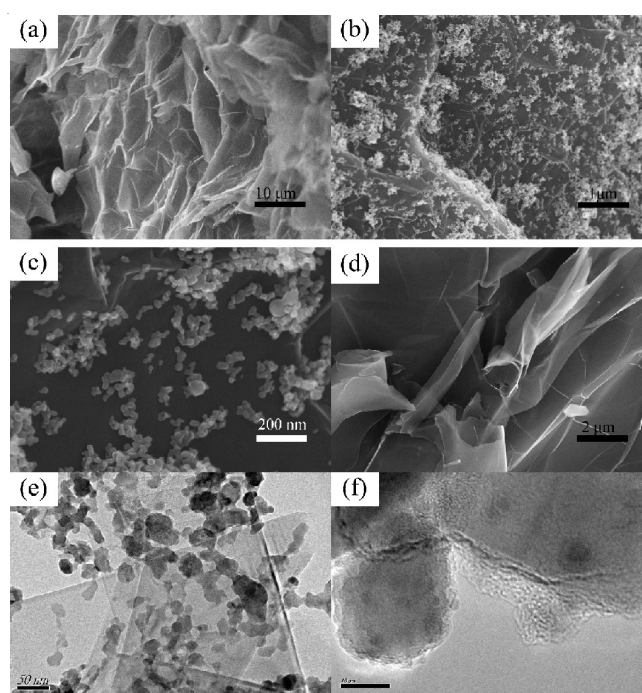


Fig. 2. SEM images of (a) EGCs without TiO_2 particles (b), (c) EGCs loaded with TiO_2 (d) the central part of C- TiO_2 /EGCs (e), (f) TEM images of EGCs loaded with TiO_2

Pore texture analysis: As shown in Fig. 3, the pore size distribution of the C-TiO₂/EGCs was calculated from N₂ adsorption isotherms. The sorption isotherms are concave to P/P₀ axis and shows typical I-type isotherm. It indicated that the C-TiO₂/EGCs were mainly made of micropores. Owing to micropore filling, high uptakes are observed at relatively low pressures.

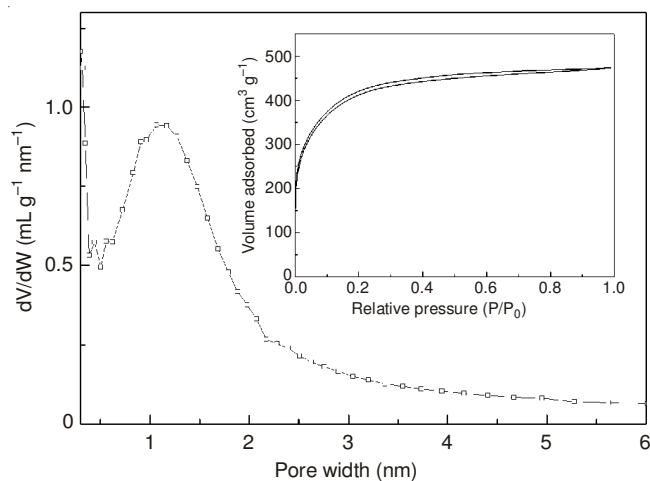


Fig. 3. Pore size distribution and adsorption isotherm of the C-TiO₂/EGCs by nitrogen adsorption

Synergetic degradation of formaldehyde: The formaldehyde reductions become more efficient in the photocatalytic oxidation process than in the adsorption process (Fig. 4). The combination of adsorption and photocatalytic oxidation achieves the maximum of the degradation process. The synergy effect between TiO₂ and EGCs using C-TiO₂/EGCs could be summarized as follows: (1) formaldehyde was adsorbed on the EGCs and carbon layer enfolded the TiO₂ nanoparticles. (2) Through the surface diffusing, formaldehyde could quickly migrate to the exterior loaded TiO₂ and the interior pores. (3) Formaldehyde was oxidized by powerful oxidizing agents that were produced from photocatalytic stimulation.

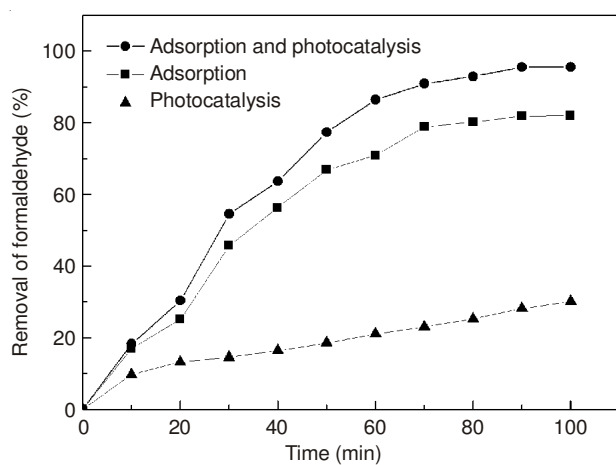


Fig. 4. Removal efficiency of formaldehyde treated by adsorption, photocatalysis and adsorption plus photocatalysis

Recycling degradation of formaldehyde: In practice, the product is often utilized for many times. So the recycling ability of C-TiO₂/EGCs to photocatalytic degradation of form-

aldehyde is very important. Fig. 5 is the repetitive tests for C-TiO₂/EGCs during photocatalytic degradation of formaldehyde with a loading of TiO₂ of 12 wt %. As shown in Fig. 6, after recycling 3 times, C-TiO₂/EGCs sample calcined can still completely degrade the formaldehyde within 100 min, suggesting that C-TiO₂/EGCs have a good reusability.

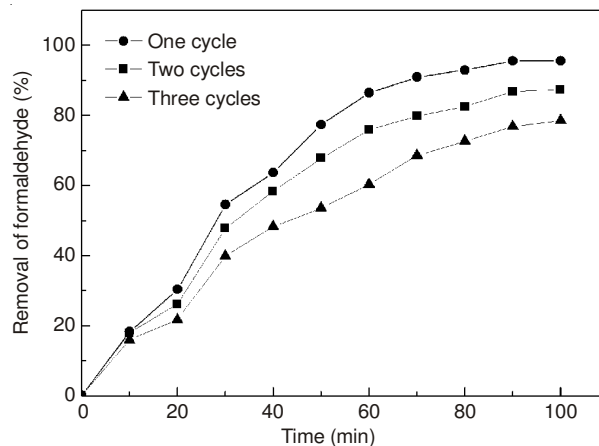


Fig. 5. Repeatability tests for C-TiO₂/EGCs during photocatalytic degradation of formaldehyde

Conclusion

Synergetic degradation research shows that the formaldehyde reduction was much more quickly in the photocatalytic oxidation process than in the adsorption process. When the loading of TiO₂ is 11.57 wt % and sucrose concentration was 0.5 %, a maximum catalytic efficiency is reached. It not only ensures the adsorption performance and realizes higher photocatalytic degradation ability of the C-TiO₂/EGCs formaldehyde treatment effect. In addition, powerful binder of TiO₂ and EGCs make ensure the recycling of the material. Carbon film was beneficial to suppress the phase transformation, so TiO₂ could retain high photocatalytic activity property even calcinated at high temperature. At the same time, the carbon coated TiO₂ with suitable carbon doping possesses visible light response capacity. Carbon film not only ensures the adsorption performance but realizes higher photocatalytic degradation ability of the formaldehyde C-TiO₂/EGCs treatment effect.

ACKNOWLEDGEMENTS

This project was financially supported by the Fundamental Research Funds for the National Natural Science Foundation of China (Nos. 21071107, 21277094 and 21103119), Production and Research Collaborative Innovation Project of Jiangsu Province (No. BY2012123), Natural Science Foundation of Jiangsu Province (No. BK2012167), Science and Technology Pillar Program (Industry) of Jiangsu Province (No. BE2012101), Collegiate Natural Science Fund of Jiangsu Province (Nos. 12KJA430005, 11KJB430012), A Project Funded by the Priority Academic Program Development of Jiangsu Higher Education Institutions (PAPD), Applied Basic Research Project of Suzhou (No. SYG201242, SYG201316), Jiangsu Key Laboratory of Material Tribology (No. Kjsmxcx2011001), Jiangsu Key Laboratory for Photon Manufacturing (No. GZ201111), Jiangsu Provincial Key Laboratory for Interventional Medical

Devices (No. Jr1210), Science and Technology Pillar Program (Industry) of Changzhou (No. CE20120067) and Creative Project of Postgraduate of Jiangsu Province (No. 856 and CXZZ13_0855).

REFERENCES

1. T. Noguchi, A. Fujishima, P. Sawunyama and K. Hashimoto, *Environ. Sci. Technol.*, **32**, 3831 (1998).
2. S. Li, F. Li and Z. Rao, *Sens. Actuators B*, **145**, 78 (2010).
3. J.R. Guimarães, C.R. Turato Farah, M.G. Maniero and P.S. Fadini, *J. Environ. Manage.*, **107**, 96 (2012).
4. M. Eiroa, C. Kennes and M.C. Veiga, *Bioresour. Technol.*, **96**, 1914 (2005).
5. J. Wang, P. Zhang, J.-Q. Qi and P.-J. Yao, *Sens. Actuators B*, **136**, 399 (2009).
6. J.R. Raji and K. Palanivelu, *Ind. Eng. Chem. Res.*, **50**, 3130 (2011).
7. K. Nakagawa, S.R. Mukai, T. Suzuki and H. Tamon, *Carbon*, **41**, 823 (2003).
8. L. Qi, J. Yu and M. Jaroniec, *Phys. Chem. Chem. Phys.*, **13**, 8915 (2011).
9. J. Yu, G. Dai, Q. Xiang and M. Jaroniec, *J. Mater. Chem.*, **21**, 1049 (2011).
10. D. Chen and R.A. Caruso, *Adv. Funct. Mater.*, **23**, 1356 (2013).
11. Y. Li, D.-S. Hwang, N.H. Lee and S.-J. Kim, *Chem. Phys. Lett.*, **404**, 25 (2005).
12. Q. Xiao, J. Zhang, C. Xiao, Z. Si and X. Tan, *Sol. Energy*, **82**, 706 (2008).
13. Z. Fei Yin, L. Wu, H. Gui Yang and Y. Hua Su, *Phys. Chem. Chem. Phys.*, **15**, 4844 (2013).
14. J. Wang, J. Wang, Q. Sun, W. Wang, Z. Yan, W. Gong and L. Min, *J. Mater. Chem.*, **19**, 6597 (2009).
15. J. Ananpattarachai, P. Kajitvichyanukul and S. Seraphin, *J. Hazard. Mater.*, **168**, 253 (2009).